Searching for Light Bosons with King and Second-King Plots Optimized for Li^+

Gordon W.F. Drake

University of Windsor
Windsor, Ontario, Canada

Collaborators

Victor Marton (undergraduate student)*
Harvir Dhindsa (undergraduate student)*

PeiPei Zhang (Wuhan WIPM)
Zong-Chao Yan (UNB, WIPM)
Ken Baldwin (Australian National University)
Don Morton (Herzberg Institute for Astrophysics)
Aaron Bondy (Ph.D. Student)

Financial Support: NSERC and SHARCnet

ECT* Workshop
March 12, 2022

OUTLINE

- Introduction and motivation.
- What is a King plot?
- Search for new physics due to an electron-neutron interaction.
- Definition of a Second-King plot for light ions such as Li^+.
- Comprehensive search for the optimum King plot in Li^+.
- Results and conclusions.

Motivation

High accuracy atomic-physics measurements at low energy
have the potential to complement or even extend
what can be learned from high-energy particle experiments.

Springer Handbook of atomic, Molecular, and Optical Physics: Chapters on Searches for New Physics

- **Tests of Fundamental Physics (QED)**
  Authors: Peter Mohr and Eite Tiesinga
  - $g-2$
  - proton size
- **Atomic Clocks and Constraints on the Fudamental Constants**
  Authors: Savely Karshenboim, Victor Flambaum and Ekkehard Peik
- **Searches for New Particles Including Dark Matter**
  Authors: Victor Flambaum and Yevgeny Stadnik
- **Searches for New Physics**
  Author: Marianna Safronova
  - Parity nonconservation in atoms
  - Electron electric dipole moment (edm)
  - Tests of CPT symmetry (particles vs. antiparticles)
  - Lorentz invariance
  - Tests of General Relativity

King Plots

- Fundamental searches are made possible by very high precision measurements of isotope shifts in sequences of isotopes.
- Optical clock transitions achieved at the few Hz level [Manovitz et al. PRL **123**, 203001 (2019)], and the possibility of measurements at the mHz level using entangled states and coherent optical spectroscopy [Micke et al., Nature **578**, 60 (2020)].
- Recent King-plot measurements in Yb may indicate evidence for an electron-neutron interaction beyond the Standard Model [Counts et al. PRL **125**, 123002 (2020)]. Other measurements in Ca and Sr.
- Analytical methods extensively developed by the NSW group [Berengut et al. Phys. Rev. Res. **2**, 043444 (2020)]. See also Müller et al. PRA **104**, L020802 (2021).
- The goal of this work is to extend King-plot methods to light atoms where second-order mass polarization effects are important. See Drake, Dhindsa and Marton, Phys. Rev. A **104**, L060801 (2021).
- All five isotopes ^{6}Li, ^{7}Li, ^{8}Li, ^{9}Li and ^{11}Li have been extensively studied and nuclear charge radii determined from the isotope shifts [see Nörtershäuser et al. PRA **83**, 012516 (2011) and Lu et al. RMP **85**, 1383 (2013)].
- For Li^{+} high precision QED theory of fine and hyperfine structure is available. See Qi et al. Phys. Rev. Lett. **125**, 183002 (2020). (Recall Wei Sun's talk from yesterday.)

PHYSICAL REVIEW A **104**, L060801 (2021)

Letter

King and second-King plots with optimized sensitivity for lithium ions

G. W. F. Drake, Harvir S. Dhindsa, and Victor J. Marton*
Department of Physics, University of Windsor, Windsor, Ontario, Canada N9B 3P4

(Received 16 September 2021; accepted 18 November 2021; published 6 December 2021)

King plots constructed from combinations of mass-weighted atomic isotope shifts provide a sensitive technique to search for electron-neutron interactions beyond the standard model mediated by a light boson. Using high-precision variational wave functions in Hylleraas coordinates, we present a comprehensive survey of all possible King plots arising from states of Li^+ up to principal quantum number $n = 10$ and angular momentum $L = 7$ in order to identify the ones most sensitive to new physics. A major limitation in previous work due to second-order mass polarization is eliminated by the introduction of a second-King plot defined in terms of second differences. The residual theoretical uncertainty is then of the order of $\alpha^2(\mu/M)^3 \sim 0.4$ Hz, where α is the fine-structure constant and μ is the reduced electron mass for a nucleus of mass M. Test results are presented for the $^A Li^+$ isotope sequence with $A = 6, 7, 8, 9, 11$ and are compared with other methods, including the Yb^+ case recently studied both experimentally and theoretically. It is shown that the second-King plots for Li^+ have about the same sensitivity to new physics as the Yb^+ case for boson masses up to about 10 keV, and nuclear size uncertainties (including nuclear polarization) are suppressed. This greatly extends the sensitivity to new physics for light two-electron systems.

DOI: 10.1103/PhysRevA.104.L060801

What is a King Plot?

- First introduced by W. H. King J. Opt. Soc. Am. **53**, 638 (1963) also W. H. King, *Isotope Shifts in Atomic Spectra* (Springer Science & Business Media, 2013).
- Provides a systematic method to look for systematic trends in atomic isotope shifts.
- Basic idea: partition the total isotope shift into a <u>mass shift</u> (atomic structure) and a <u>field shift</u> (nuclear size and structure).
- Let i and j denote two atomic states, and a a particular isotope. The transition frequency between states i an j can then be expanded in the form

$$\nu_a^{ij} = U^{ij} + \underbrace{V^{ij}\left(\frac{\mu}{M}\right)_a + W^{ij}\left(\frac{\mu}{M}\right)_a^2 + \cdots}_{\text{mass shift}} + \underbrace{C^{ij}\bar{r}_a^2}_{\text{field shift}} \tag{1}$$

where

$U^{ij} = (E^i - E^j)/\hbar$ for an infinitely heavy point nucleus (incl. relativistic and QED)
$V^{ij} =$ normal and specific mass shifts (incl. relativistic and QED)
$W^{ij} =$ second-order mass shifts (incl. relativistic and QED)
$C^{ij} = \frac{2\pi Z e^2}{3} \sum_k [\langle \delta(\mathbf{r}_k)\rangle_i - \langle \delta(\mathbf{r}_k)\rangle_j]$
$\bar{r}_a^2 =$ mean square nuclear charge radius

- The isotope shift between two different isotopes a and b is then

$$\nu_a^{ij} - \nu_b^{ij} = \underbrace{V^{ij}\left[\left(\frac{\mu}{M}\right)_a - \left(\frac{\mu}{M}\right)_b\right] + W^{ij}\left[\left(\frac{\mu}{M}\right)_a^2 - \left(\frac{\mu}{M}\right)_b^2\right] + \cdots}_{\text{mass shift}} + \underbrace{C^{ij}(\bar{r_a^2} - \bar{r_b^2})}_{\text{field shift}}$$

Divide by $\left(\frac{\mu}{M}\right)_a - \left(\frac{\mu}{M}\right)_b$ to obtain the King coordinate

$$\begin{aligned} n_{ab}^{ij} &= \frac{\nu_a^{ij} - \nu_b^{ij}}{\left(\frac{\mu}{M}\right)_a - \left(\frac{\mu}{M}\right)_b} \\ &= V^{ij} + W^{ij}\left[\left(\frac{\mu}{M}\right)_a + \left(\frac{\mu}{M}\right)_b\right] + \cdots + \frac{C^{ij}(\bar{r_a^2} - \bar{r_b^2})}{\left(\frac{\mu}{M}\right)_a - \left(\frac{\mu}{M}\right)_b} \end{aligned}$$

See example King plot.

- A third isotope c defines a King slope

$$\begin{aligned} S_{bc} &= \frac{n_{ac}^{i'j'} - n_{ab}^{i'j'}}{n_{ac}^{ij} - n_{ab}^{ij}} \\ &\to \frac{C^{i'j'}}{C^{ij}} \quad \text{if } W^{i'j'} = W^{ij} = 0 \\ &\equiv \frac{\sum_k[\langle\delta(\mathbf{r}_k)\rangle_{i'} - \langle\delta(\mathbf{r}_k)\rangle_{j'}]}{\sum_k[\langle\delta(\mathbf{r}_k)\rangle_i - \langle\delta(\mathbf{r}_k)\rangle_j]} \end{aligned}$$

- If c is replaced by a fourth isotope d, then there should be no change in slope.

King Plot

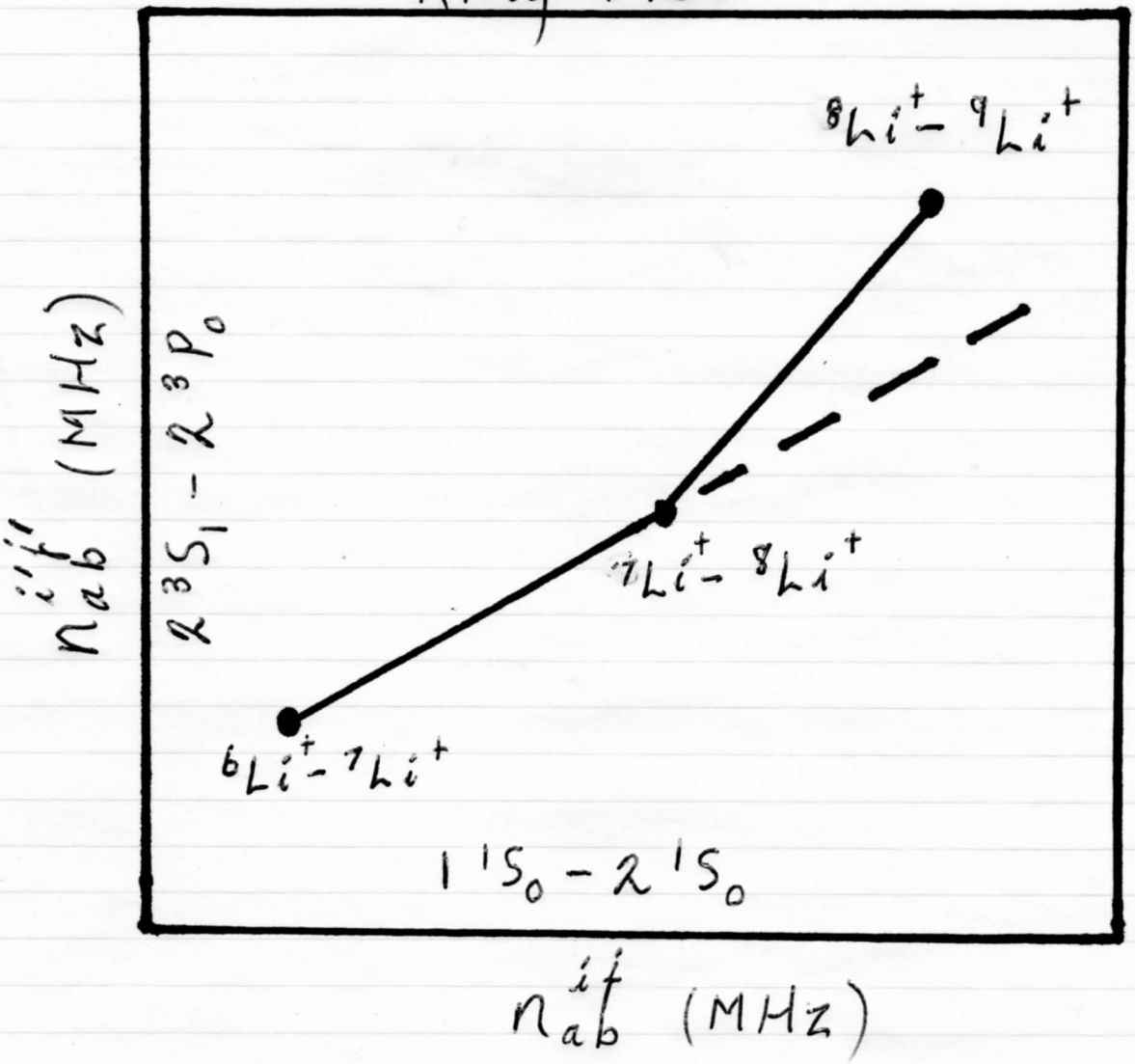
$^8Li^+ - {}^9Li^+$
$^7Li^+ - {}^8Li^+$
$^6Li^+ - {}^7Li^+$
n_{ab}^{if} (MHz)
$2\,^3S_1 - 2\,^3P_0$
$1\,^1S_0 - 2\,^1S_0$
n_{ab}^{if} (MHz)

- The isotope shift between two different isotopes a and b is then

$$\nu_a^{ij} - \nu_b^{ij} = \underbrace{V^{ij}\left[\left(\frac{\mu}{M}\right)_a - \left(\frac{\mu}{M}\right)_b\right] + W^{ij}\left[\left(\frac{\mu}{M}\right)_a^2 - \left(\frac{\mu}{M}\right)_b^2\right] + \cdots}_{\text{mass shift}} + \underbrace{C^{ij}(\bar{r_a^2} - \bar{r_b^2})}_{\text{field shift}}$$

Divide by $\left(\frac{\mu}{M}\right)_a - \left(\frac{\mu}{M}\right)_b$ to obtain the King coordinate

$$\begin{aligned} n_{ab}^{ij} &= \frac{\nu_a^{ij} - \nu_b^{ij}}{\left(\frac{\mu}{M}\right)_a - \left(\frac{\mu}{M}\right)_b} \\ &= V^{ij} + W^{ij}\left[\left(\frac{\mu}{M}\right)_a + \left(\frac{\mu}{M}\right)_b\right] + \cdots + \frac{C^{ij}(\bar{r_a^2} - \bar{r_b^2})}{\left(\frac{\mu}{M}\right)_a - \left(\frac{\mu}{M}\right)_b} \end{aligned}$$

See example King plot.

- A third isotope c defines a King slope

$$\begin{aligned} S_{bc} &= \frac{n_{ac}^{i'j'} - n_{ab}^{i'j'}}{n_{ac}^{ij} - n_{ab}^{ij}} \\ &\to \frac{C^{i'j'}}{C^{ij}} \quad \text{if } W^{i'j'} = W^{ij} = 0 \\ &\equiv \frac{\sum_k[\langle\delta(\mathbf{r}_k)\rangle_{i'} - \langle\delta(\mathbf{r}_k)\rangle_{j'}]}{\sum_k[\langle\delta(\mathbf{r}_k)\rangle_i - \langle\delta(\mathbf{r}_k)\rangle_j]} \end{aligned}$$

- If c is replaced by a fourth isotope d, then there should be no change in slope.

Searches for New Physics

There are (at least) three sources of nonlinearity in the King plot:

1. For light atoms such as He and Li^+, the term $W^{ij}\left[\left(\frac{\mu}{M}\right)_a + \left(\frac{\mu}{M}\right)_b\right]$ is not small.
2. There are higher-order corrections to the field shift term.
3. There is an additional electron-neutron interaction due to exchange of light bosons beyond the Standard Model.

Item #1 can be handled by taking second differences to eliminate the W^{ij} term to form a second-King plot, or by means of generalized King plots, as discussed by Berengut et al. Phys. Rev. Research **2**, 043444 (2020), and similarly for item #2.

Nuclear size uncertainties were recently discussed by Müller et al. Phys. Rev. A **104**, L020802 (2021).

Item #3 is the principal topic of the present work.

New Light Bosons

- As discussed by Delaunay et al. [PRD **96**,093001 (2017)] a possible candidate for dark matter is a light boson that propagates an electron-neutron interaction. It depends on the number of neutrons in the nucleus, and so varies from one isotope to the next, just as the electric field varies with the number of protons. The corresponding hypothetical Yukawa potential is

$$V_{m_\phi} = \frac{N_I y_e y_n}{4\pi r} e^{-\gamma r}$$

  where $\gamma = 1/\alpha a_{m_\phi}$ and αa_{m_ϕ} is the Compton wavelength for the boson of mass m_ϕ, $a_{m_\phi} = \hbar^2/(m_\phi e^2)$ is the corresponding Bohr radius, $y_e y_n/(4\pi)$ is a coupling constant and N_I is the number of neutrons for isotope I, analogous to $Ze^2/(4\pi\epsilon_0)$ for then electron-nucleus interaction.

- The boson must be "light" because otherwise the range is too short and the potential looks like a delta-function that is indistinguishable from the regular nuclear potential.

- The useful mass range is therefore from 0 up to about 10 keV.

- If present, it would produce a kink in the King plot.

Modified King Plot

Ignore for now the W^{ij} quadratic mass-polarization term, and extend the King coordinate to read

$$n_{ab}^{ij} = V^{ij} + C^{ij} G_{ab} + \Upsilon^{ij} N_{ab}$$

where

$$N_{ab} = \frac{N_a - N_b}{\left(\frac{\mu}{M}\right)_a - \left(\frac{\mu}{M}\right)_b}, \quad G_{ab} = \frac{\bar{r}_a^2 - \bar{r}_b^2}{\left(\frac{\mu}{M}\right)_a - \left(\frac{\mu}{M}\right)_b}$$

and Υ^{ij} denotes the difference in matrix elements of the Yukawa potential

$$\Upsilon^{ij} = \langle i | V_{m_\phi} | i \rangle - \langle j | V_{m_\phi} | j \rangle$$

For the King plot with a third isotope c it is convenient to define

$$\Delta N_{bc} = N_{ab} - N_{ac}, \quad \Delta G_{bc} = G_{ab} - G_{ac}$$

Then after some algebra, the change in slope if c is replaced by a fourth isotope d is

$$\Delta S_{cd} = \frac{C^{i'j'}}{C^{ij}} \left(\frac{\Upsilon^{i'j'}}{C^{i'j'}} - \frac{\Upsilon^{ij}}{C^{ij}} \right) \left(\frac{\Delta N_{bd}}{\Delta G_{bd}} - \frac{\Delta N_{bc}}{\Delta G_{bc}} \right)$$

- Doesn't work for Li^+ because the W^{ij} mass-polarization term is too large.
- Cure: take second differences to eliminate the W^{ij} term.

Second-King Plots

For light ions, the W^{ij} term can be eliminated by forming the second-King coordinate

$$\kappa^{ij}_{abc} = \frac{n^{ij}_{ab} - n^{ij}_{ac}}{\left(\frac{\mu}{M}\right)_b - \left(\frac{\mu}{M}\right)_c} \tag{2}$$

Then, with the definition

$$\begin{aligned} Q_{abc} \;=\; & \frac{\bar{r}^2_a}{\left[\left(\frac{\mu}{M}\right)_a - \left(\frac{\mu}{M}\right)_b\right]\left[\left(\frac{\mu}{M}\right)_a - \left(\frac{\mu}{M}\right)_c\right]} \\ & + \frac{\bar{r}^2_b}{\left[\left(\frac{\mu}{M}\right)_b - \left(\frac{\mu}{M}\right)_a\right]\left[\left(\frac{\mu}{M}\right)_b - \left(\frac{\mu}{M}\right)_c\right]} \\ & + \frac{\bar{r}^2_c}{\left[\left(\frac{\mu}{M}\right)_c - \left(\frac{\mu}{M}\right)_a\right]\left[\left(\frac{\mu}{M}\right)_c - \left(\frac{\mu}{M}\right)_b\right]} \end{aligned} \tag{3}$$

Eq. (2) becomes

$$\kappa^{ij}_{abc} = W^{ij} + C^{ij} Q_{abc} \tag{4}$$

Factors of $Q_{abc} - Q_{abd}$ then cancel from numerator and denominator of the second-King slope defined by

$$S^{(2)} = \frac{\kappa^{i'j'}_{abc} - \kappa^{i'j'}_{abd}}{\kappa^{ij}_{abc} - \kappa^{ij}_{abd}} \tag{5}$$

leaving $S^{(2)} = \frac{C^{i'j'}}{C^{ij}}$, which is the same as for the standard King slope. The disadvantage of course is that one needs a sequence five isotopes instead of four to look for a change in slope due to new physics BSM.

Second-King plot to search for new physics BSM

With an additional boson interaction, the modified second-King coordinate becomes

$$\kappa^{ij}_{abc} = W^{ij} + C^{ij} Q_{abc} + \Upsilon^{ij} N_{abc} \tag{6}$$

where, in parallel with Q_{abc}

$$\begin{aligned} N_{abc} &= \frac{N_a}{\left[\left(\frac{\mu}{M}\right)_a - \left(\frac{\mu}{M}\right)_b\right]\left[\left(\frac{\mu}{M}\right)_a - \left(\frac{\mu}{M}\right)_c\right]} \\ &+ \frac{N_b}{\left[\left(\frac{\mu}{M}\right)_b - \left(\frac{\mu}{M}\right)_a\right]\left[\left(\frac{\mu}{M}\right)_b - \left(\frac{\mu}{M}\right)_c\right]} \\ &+ \frac{N_c}{\left[\left(\frac{\mu}{M}\right)_c - \left(\frac{\mu}{M}\right)_a\right]\left[\left(\frac{\mu}{M}\right)_c - \left(\frac{\mu}{M}\right)_b\right]} \end{aligned} \tag{7}$$

and N_a, N_b and N_c are the neutron numbers for isotopes a, b, c respectively. Note that $N_{abc} = 0$ if $\{N_a, N_b, N_c\}$ are all equal, and so it depends only on the *change* in neutron number.

For brevity, define $\Delta Q_{cd} = Q_{abc} - Q_{abd}$ and $\Delta N_{cd} = N_{abc} - N_{abd}$. Once again the W^{ij} term cancels from the slope of the second-King plot, resulting in

$$\begin{aligned} S^{(2)} &= \frac{C^{i'j'}\Delta Q_{cd} + \Upsilon^{i'j'}\Delta N_{cd}}{C^{ij}\Delta Q_{cd} + \Upsilon^{ij}\Delta N_{cd}} \\ &\simeq \frac{C^{i'j'}}{C^{ij}}\left[1 + \left(\frac{\Upsilon^{i'j'}}{C^{i'j'}} - \frac{\Upsilon^{ij}}{C^{ij}}\right)\frac{\Delta N_{cd}}{\Delta Q_{cd}}\right] \end{aligned} \tag{8}$$

assuming in the second line that the Υ^{ij} term is small so that the denominator can be expanded into the numerator.

Finally, if the isotope d is replaced by a fifth isotope e, then the change in slope is

$$\Delta S^{(2)}_{de} = \frac{C^{i'j'}}{C^{ij}} \left(\frac{\Upsilon^{i'j'}}{C^{i'j'}} - \frac{\Upsilon^{ij}}{C^{ij}} \right) \left(\frac{\Delta N_{ce}}{\Delta Q_{ce}} - \frac{\Delta N_{cd}}{\Delta Q_{cd}} \right) \tag{9}$$

This shows a clear factorization into a part determined by the nuclear properties represented by the last factor, and a part determined by the electronic wave function represented by the first two factors. It is a nonzero value for the middle factor that would represent a signal for new physics BSM.

Sensitivity to New Physics

Assume a 1 Hz uncertainty in each of the four isotope shift measurements required to determine a King slope. The sensitivity is then defined as the value of the boson coupling constant $y_e y_n$ for which

$$\Delta S^{(2)}_{de} / S^{(2)} = \Delta S^{(2)}_{1\mathrm{Hz}} / S^{(2)}$$

where $\Delta S^{(2)}_{1\mathrm{Hz}}$ is the uncertainty in $S^{(2)}$ induced by the 1 Hz measurement uncertainties added in quadrature.

Nonrelativistic Eigenvalues

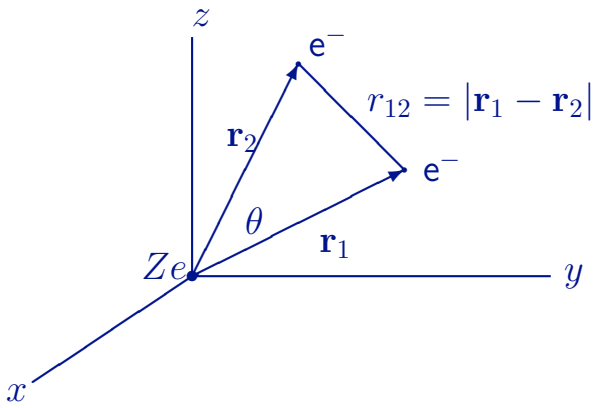

Hylleraas coordinates

(Hylleraas, 1929)

The Hamiltonian in atomic units is

$$H = -\frac{1}{2}\nabla_1^2 - \frac{1}{2}\nabla_2^2 - \frac{Z}{r_1} - \frac{Z}{r_2} + \frac{1}{r_{12}}$$

Expand

$$\Psi(\mathbf{r}_1, \mathbf{r}_2) = \sum_{i,j,k} a_{ijk}\, r_1^i\, r_2^j\, r_{12}^k\, e^{-\alpha r_1 - \beta r_2}\, \mathcal{Y}_{l_1 l_2 L}^M(\hat{\mathbf{r}}_1, \hat{\mathbf{r}}_2) \pm \text{exchange}$$

where $i + j + k \leq \Omega$ (Pekeris shell).

Diagonalize H in the

$$\phi_{ijk} = r_1^i\, r_2^j\, r_{12}^k\, e^{-\alpha r_1 - \beta r_2}\, \mathcal{Y}_{l_1 l_2 L}^M(\hat{\mathbf{r}}_1, \hat{\mathbf{r}}_2) \pm \text{exchange}$$

basis set.

to satisfy the variational condition

$$\delta \int \Psi\, (H - E)\, \Psi\, d\tau = 0.$$

New Variational Techniques

I. Double the basis set

$$\begin{aligned} \text{If} \quad \phi_{i,j,k}(\alpha,\beta) &= r_1^i r_2^j r_{12}^k e^{-\alpha r_1 - \beta r_2} \\ \text{then} \quad \tilde{\phi}_{i,j,k} &= \underbrace{a_1 \phi_{i,j,k}(\alpha_1,\beta_1)}_{\text{asymptotic}} + \underbrace{a_2 \phi_{i,j,k}(\alpha_2,\beta_2)}_{\text{inner correlation}} \end{aligned}$$

II. Include the screened hydrogenic function

$$\phi_{\mathsf{SH}} = \psi_{1s}(Z)\psi_{nL}(Z-1)$$

explicitly in the basis set.

III. Optimize the nonlinear parameters

$$\begin{aligned} \frac{\partial E}{\partial \alpha_t} &= -2\langle \Psi_{\mathsf{tr}} \mid H - E \mid r_1 \Psi(\mathbf{r}_1,\mathbf{r}_2;\alpha_t) \pm r_2 \Psi(\mathbf{r}_2,\mathbf{r}_1;\alpha_t)\rangle \\ \frac{\partial E}{\partial \beta_t} &= -2\langle \Psi_{\mathsf{tr}} \mid H - E \mid r_2 \Psi(\mathbf{r}_1,\mathbf{r}_2;\alpha_t) \pm r_1 \Psi(\mathbf{r}_2,\mathbf{r}_1;\alpha_t)\rangle \end{aligned}$$

for $t = 1$, 2, with $\langle \Psi_{\mathsf{tr}} \mid \Psi_{\mathsf{tr}} \rangle = 1$.
$\Psi(\mathbf{r}_1,\mathbf{r}_2;\alpha_t) =$ terms in Ψ_{tr} which depend explicitly on α_t.

For all states up to $n = 10$ and $L = 7$, see Drake and Yan, PRA **46**, 2378 (1992) and http://drake.sharcnet.ca for downloadable resources.

Mass Scaling

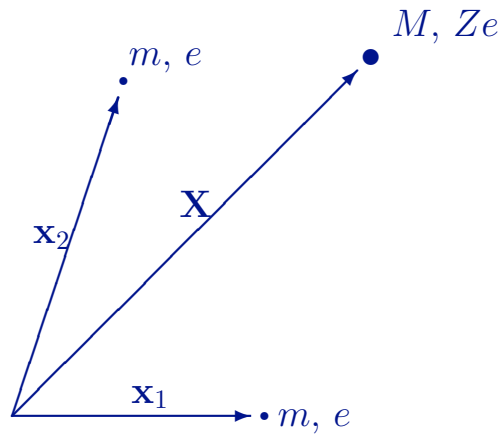

$$H = -\frac{\hbar^2}{2M}\nabla_X^2 - \frac{\hbar^2}{2m}\nabla_{x_1}^2 - \frac{\hbar^2}{2m}\nabla_{x_2}^2 - \frac{Ze^2}{|\mathbf{X}-\mathbf{x}_1|} - \frac{Ze^2}{|\mathbf{X}-\mathbf{x}_2|} + \frac{e^2}{|\mathbf{x_1}-\mathbf{x}_2|}$$

Transform to centre-of-mass plus relative coordinates $\mathbf{R}$, $\mathbf{r}_1$, $\mathbf{r}_2$

$$\begin{aligned}
\mathbf{R} &= \frac{M\mathbf{X} + m\mathbf{x}_1 + m\mathbf{x}_2}{M+2m} \\
\mathbf{r}_1 &= \mathbf{X} - \mathbf{x}_1 \\
\mathbf{r}_2 &= \mathbf{X} - \mathbf{x}_2
\end{aligned}$$

and ignore centre-of-mass motion. Then

$$H = -\frac{\hbar^2}{2\mu}\nabla_{r_1}^2 - \frac{\hbar^2}{2\mu}\nabla_{r_2}^2 - \frac{\hbar^2}{M}\nabla_{r_1}\cdot\nabla_{r_2} - \frac{Ze^2}{r_1} - \frac{Ze^2}{r_2} + \frac{e^2}{|\mathbf{r_1}-\mathbf{r}_2|}$$

where $\mu = \dfrac{mM}{m+M}$ is the electron reduced mass.

Expand

$$\begin{aligned}\Psi &= \Psi_0 + \frac{\mu}{M}\Psi_1 + \left(\frac{\mu}{M}\right)^2 \Psi_2 + \cdots \\ \mathcal{E} &= \mathcal{E}_0 + \frac{\mu}{M}\mathcal{E}_1 + \left(\frac{\mu}{M}\right)^2 \mathcal{E}_2 + \cdots\end{aligned}$$

The zero-order problem is the Schrödinger equation for infinite nuclear mass

$$\left\{-\frac{1}{2}\nabla^2_{\rho_1} - \frac{1}{2}\nabla^2_{\rho_2} - \frac{Z}{\rho_1} - \frac{Z}{\rho_2} + \frac{1}{|\boldsymbol{\rho}_1 - \boldsymbol{\rho}_2|}\right\}\Psi_0 = \mathcal{E}_0\Psi_0$$

The "normal" isotope shift is

$$\Delta E_{\text{normal}} = -\frac{\mu}{M}\left(\frac{\mu}{m}\right)\mathcal{E}_0 \quad 2R_\infty$$

The first-order "specific" isotope shift is

$$\Delta E^{(1)}_{\text{specific}} = -\frac{\mu}{M}\left(\frac{\mu}{m}\right)\langle\Psi_0|\nabla_{\rho_1}\cdot\nabla_{\rho_2}|\Psi_0\rangle \quad 2R_\infty$$

The second-order "specific" isotope shift is

$$\Delta E^{(2)}_{\text{specific}} = \left(-\frac{\mu}{M}\right)^2\left(\frac{\mu}{m}\right)\langle\Psi_0|\nabla_{\rho_1}\cdot\nabla_{\rho_2}|\Psi_1\rangle \quad 2R_\infty$$

ASYMPTOTIC EXPANSION FOR $\langle \delta(r_1) + \delta(r_2) \rangle$

Core Polarization Model (Dalgarno, Drachman)

– neglect exchange.
– Rydberg electron moves in the field generated by the polarizable core.

$$V(x) = -\frac{Z-1}{x} + \Delta V(x)$$

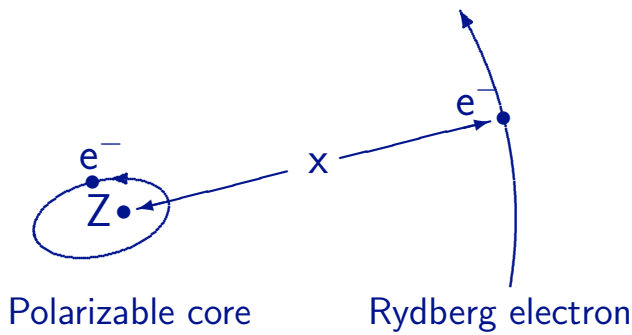

Illustration of the physical basis for the asymptotic expansion method in which the Rydberg electron moves in the field generated by the polarized core.

$$\Delta V(x) = -\frac{c_4}{x^4} - \frac{c_6}{x^6} - \frac{c_7}{x^7} - \frac{c_8}{x^8} - \frac{c_9}{x^9} - \frac{c_{10}}{x^{10}} + \cdots$$

For example, $c_4 = \frac{1}{2}\alpha_1$
$c_6 = \frac{1}{2}(\alpha_2 - 6\beta_1)$

where

$$\alpha_1 = \frac{9}{2Z^4} \text{ is the dipole polarizability,}$$

$$\alpha_2 = \frac{15}{Z^6} \text{ is the quadrupole polarizability,}$$

$$\beta_1 = \frac{43}{8Z^6} \text{ is a nonadiabatic correction.}$$

For the δ-function [Drake, PRA **45**, 70 (1992)]

$$\langle\delta(\mathbf{r}_1)\rangle = \frac{Z^3}{\pi a_\mu^3}\left[\frac{1}{2} - \frac{62}{Z^6}\langle x^{-4}\rangle_{nL} + \frac{1447}{4Z^8}\langle x^{-6}\rangle_{nL} + \cdots\right]$$

and the finite mass correction due to mass polarization is

$$\Delta\langle\delta(\mathbf{r}_1)\rangle = \frac{Z^3}{\pi a_\mu^3}\left(\frac{\mu}{M}\right)\left[-\frac{124}{Z^6}\langle x^{-4}\rangle_{nL} + \frac{4789}{2Z^8}\langle x^{-6}\rangle_{nL} + \cdots\right]$$

All calculations can be done analytically, using methods of Dalgarno and Stewart (1956-60) and Cohen and Dalgarno (1961-66), especially the "Dalgarno Interchange Theorem."

See G.W.F. Drake, Adv. At. Mol. Opt. Phys. **31**, 1 (1993).

$$\langle x^{-4}\rangle_{nL} = \frac{16(Z-1)^4[3n^2 - L(L+1)]}{n^5(2L+3)(2L+2)(2L+1)(2L)(2L-1)}$$

TABLE II. Comparison of values for $\pi\langle\delta(\mathbf{r})\rangle - 4$ (units of 10^{-6} a.u.). [Drake, PRA 45, 70 (1992)]

		Variational calculation			
L	n	Singlet	Triplet	Asymptotic expansion	Difference[a]
3	4	−35.183 0(1)[b]	−35.397 3(1)	−35.6(6)	0.3(6)
3	5	−20.052 7(3)	−20.232 5(4)	−20.3(4)	0.2(4)
3	6	−12.244 7(1)	−12.373 2(2)	−12.42(27)	0.11(27)
3	7	−7.953 6(2)	−8.044 6(3)	−8.07(19)	0.07(19)
3	8	−5.433 73(4)	−5.499 2(1)	−5.52(13)	0.05(13)
3	9	−3.867 2(1)	−3.915 33(2)	−3.93(10)	0.04(10)
3	10	−2.845 3(4)	−2.881 82(2)	−2.89(7)	0.03(7)
4	5	−4.886 44(2)	−4.886 78(1)	−4.886 6(22)	0.000 0(22)
4	6	−3.135 6(1)	−3.135 9(1)	−3.136 0(25)	0.000 2(25)
4	7	−2.091 7(3)	−2.091 7(3)	−2.091 8(22)	0.000 1(22)
4	8	−1.452 0(1)	−1.452 3(1)	−1.452 2(18)	0.000 1(18)
4	9	−1.044 27(1)	−1.044 47(1)	−1.044 4(14)	0.000 0(14)
4	10	−0.774 00(1)	−0.774 12(2)	−0.774 1(11)	0.000 0(11)
5	6	−1.003 9(2)	−1.004 0(2)	−1.003 93(1)	−0.000 0(2)
5	7	−0.696 15(2)	−0.696 16(2)	−0.696 13(2)	−0.000 02(2)
5	8	−0.494 16(1)	−0.494 15(1)	−0.494 14(3)	−0.000 02(3)
5	9	−0.360 3(2)	−0.360 3(2)	−0.360 43(3)	0.000 10(20)
5	10	−0.269 71(7)	−0.269 65(6)	−0.269 72(2)	0.000 04(9)
6	7	−0.268 36(1)	−0.268 37(1)	−0.268 369(3)	0.000 004(14)
6	8	−0.196 56(1)	−0.196 56(2)	−0.196 564(1)	0.000 004(22)
6	9	−0.146 11(4)	−0.146 11(3)	−0.146 131(1)	0.000 021(50)
6	10	−0.110 74(1)	−0.110 75(1)	−0.110 741(1)	−0.000 004(15)
7	8	−0.086 575(3)	−0.086 575(3)	−0.086 575 2(5)	0.000 000 2(42)
7	9	−0.066 047 8(3)	−0.066 048 3(6)	−0.066 046 0(4)	−0.000 002 0(8)
7	10	−0.050 881(3)	−0.050 881(3)	−0.050 880 4(3)	−0.000 000 6(42)
8	9			−0.032 155 8(1)	
8	10			−0.025 314 1(1)	

[a]Difference between the singlet-triplet average and the asymptotic value.

TABLE II. Comparison of values for $\pi\langle\delta(\mathbf{r})\rangle - 4$ (units of 10^{-6} a.u.). [Drake, PRA 45, 70 (1992)]

		Variational calculation			
L	n	Singlet	Triplet	Asymptotic expansion	Difference[a]
3	4	−35.183 0(1)[b]	−35.397 3(1)	−35.6(6)	0.3(6)
3	5	−20.052 7(3)	−20.232 5(4)	−20.3(4)	0.2(4)
3	6	−12.244 7(1)	−12.373 2(2)	−12.42(27)	0.11(27)
3	7	−7.953 6(2)	−8.044 6(3)	−8.07(19)	0.07(19)
3	8	−5.433 73(4)	−5.499 2(1)	−5.52(13)	0.05(13)
3	9	−3.867 2(1)	−3.915 33(2)	−3.93(10)	0.04(10)
3	10	−2.845 3(4)	−2.881 82(2)	−2.89(7)	0.03(7)
4	5	−4.886 44(2)	−4.886 78(1)	−4.886 6(22)	0.000 0(22)
4	6	−3.135 6(1)	−3.135 9(1)	−3.136 0(25)	0.000 2(25)
4	7	−2.091 7(3)	−2.091 7(3)	−2.091 8(22)	0.000 1(22)
4	8	−1.452 0(1)	−1.452 3(1)	−1.452 2(18)	0.000 1(18)
4	9	−1.044 27(1)	−1.044 47(1)	−1.044 4(14)	0.000 0(14)
4	10	−0.774 00(1)	−0.774 12(2)	−0.774 1(11)	0.000 0(11)
5	6	−1.003 9(2)	−1.004 0(2)	−1.003 93(1)	−0.000 0(2)
5	7	−0.696 15(2)	−0.696 16(2)	−0.696 13(2)	−0.000 02(2)
5	8	−0.494 16(1)	−0.494 15(1)	−0.494 14(3)	−0.000 02(3)
5	9	−0.360 3(2)	−0.360 3(2)	−0.360 43(3)	0.000 10(20)
5	10	−0.269 71(7)	−0.269 65(6)	−0.269 72(2) <---	0.000 04(9)
6	7	−0.268 36(1)	−0.268 37(1)	−0.268 369(3) <---	0.000 004(14)
6	8	−0.196 56(1)	−0.196 56(2)	−0.196 564(1)	0.000 004(22)
6	9	−0.146 11(4)	−0.146 11(3)	−0.146 131(1)	0.000 021(50)
6	10	−0.110 74(1)	−0.110 75(1)	−0.110 741(1)	−0.000 004(15)
7	8	−0.086 575(3)	−0.086 575(3)	−0.086 575 2(5)	0.000 000 2(42)
7	9	−0.066 047 8(3)	−0.066 048 3(6)	−0.066 046 0(4)	−0.000 002 0(8)
7	10	−0.050 881(3)	−0.050 881(3)	−0.050 880 4(3)	−0.000 000 6(42)
8	9			−0.032 155 8(1)	
8	10			−0.025 314 1(1)	

[a]Difference between the singlet-triplet average and the asymptotic value.

TABLE IV. Comparison of values for the specific-mass correction to $\pi\langle\delta(\mathbf{r})\rangle$ (units of $10^{-6}\ \mu/M$ a.u.). [Drake, PRA 45, 70 (1992)]

		Variational calculation			
L	n	Singlet	Triplet	Asymptotic expansion	Difference[a]
3	4	−67(2)	−64(2)	−68.8(3.6)	3.3(4.6)
3	5	−39(1)	−36(1)	−38.9(2.7)	1.4(3.0)
3	6	−23(1)	−21(2)	−23.7(1.8)	1.7(2.9)
3	7	−16(1)	−13(1)	−15.3(1.2)	0.8(1.9)
3	8	−10(1)	−8(2)	−10.5(9)	1.5(24)
3	9	−7.0(4)	−6.5(2)	−7.4(6)	0.7(7)
3	10	−5.1(4)	−4.3(4)	−5.5(5)	0.8(8)
4	5	−9.3(6)	−9.2(6)	−9.61(1)	0.4(8)
4	6	−6.0(7)	−6.1(2)	−6.13(1)	0.1(7)
4	7	−3.9(2)	−3.6(2)	−4.08(1)	0.3(3)
4	8	−3.2(4)	−3.5(7)	−2.828(8)	0.5(8)
4	9	−2.7(1.0)	−2.2(5)	−2.031(6)	−0.4(1.1)
4	10	−1.6(4)	−1.5(4)	−1.505(5)	−0.5(6)
5	6	−2.0(3)	−2.1(2)	−1.994 9(3)	−0.05(36)
5	7	−1.4(1)	−1.4(1)	−1.380 5(4)	−0.02(14)
5	8	−0.9(4)	−1.0(4)	−0.978 8(3)	0.03(56)
5	9	−0.6(4)	−0.5(4)	−0.713 4(3)	0.16(56)
5	10	−0.57(5)	−0.59(2)	−0.533 6(2)	−0.05(6)
6	7	−0.56(7)	−0.55(5)	−0.535 14(2)	−0.02(8)
6	8	−0.35(2)	−0.31(5)	−0.391 61(2)	0.06(5)
6	9	−0.27(1)	−0.27(1)	−0.290 97(2)	0.02(2)
6	10	−0.16(5)	−0.17(5)	−0.220 42(2)	0.05(8)
7	8	−0.17(1)	−0.18(2)	−0.172 879(2)	0.003(22)
7	9	−0.131(2)	−0.126(6)	−0.131 825(2)	−0.004(6)
7	10	−0.103(3)	−0.103(2)	−0.101 525(2)	−0.002(4)
8	9			−0.064 253 6(2)	
8	10			−0.050 569 7(3)	

[a]Difference between the singlet-triplet average and the asymptotic value.

Results

- Comprehensive survey of all possible King plots for states of Li^+ up to $n = 10$ and $L = 7$ (K-states).
- Counting both singlets and triplets, there are $N_S = 103$ states in this range.
- The number of possible unique King plots is

$$\begin{aligned} N_{\mathrm{King}} &= \frac{1}{8} N_S (N_S - 1)[N_S(N_S - 1) - 2] \\ &= 13\,794\,378 \end{aligned}$$

- Assume a nominal 1 Hz accuracy in the isotope shift measurements.

Contributions to the slope of the regular King plots k1, k2, and k3, and the second-King (super-King) plots k1$^{(2)}$ and k2$^{(2)}$ for the transition pair $2\ ^3P_1 - 10\ ^3S_1/2\ ^3S_1 - 10\ ^3S_1$ of Li$^+$. The last line is the uncertainty in the slope induced by a ± 1 Hz uncertainty in each of the independent isotope shift measurements.

Contribution	k1	k2	k3	k1$^{(2)}$	k2$^{(2)}$
Infinite mass limit	–3.453 226	–3.453 226	–3.453 226	–3.453 226	–3.453 226
$(\mu/M)^2 + \cdots$	4.101 441	4.446 124	2.328 237	0.000 153	0.000 082
$(\mu/M)\bar{r}_c^2$	0.000 208	0.000 154	0.000 456	0.000 816	0.000 859
Total	0.648 423	0.993 052	–1.124 533	–3.452 257	–3.452 285
Nucl. radius uncertainty	$\pm$0.56	$\pm$0.31	$\pm$0.06	$\pm$0.000 037	$\pm$0.000 012
± 1 Hz	0.000 002	0.000 001	0.000 001	0.000 009	0.000 005

Transitions with highest sensitivity to electron-neutron interactions for different vales of the Yukawa parameter γ. The conversion factor from γ to boson mass m_ϕ is $Z\alpha m_e = 11.1868$ keV with $Z = 3$.

γ (Z/a_0)	King transitions	$y_e y_n$
0.001	$2\,^1S$-$10\,^1S/2\,^3P$-$10\,^1S$	9.6312×10^{-15}
0.002	$2\,^1S$-$10\,^1S/2\,^3P$-$10\,^1S$	9.6465×10^{-15}
0.005	$2\,^1S$-$10\,^1S/2\,^3P$-$10\,^1S$	9.7322×10^{-15}
0.010	$2\,^3P$-$10\,^3S/2\,^1S$-$10\,^1S$	9.9455×10^{-15}
0.020	$2\,^1P$-$5\,^3S/2\,^1P$-$7\,^1S$	1.0363×10^{-14}
0.050	$2\,^1P$-$5\,^3S/2\,^1P$-$7\,^1S$	1.2040×10^{-14}
0.100	$2\,^1P$-$5\,^3S/2\,^1P$-$7\,^1S$	1.5689×10^{-14}
0.200	$2\,^1S$-$10\,^1S/2\,^3P$-$10\,^3S$	2.5312×10^{-14}
0.200	$2\,^1S$-$10\,^3S/2\,^3P$-$10\,^3S$	2.5307×10^{-14}
0.500	$2\,^3P$-$2\,^3S/1\,^1S$-$2\,^1S$ [a]	5.4886×10^{-14}
1.000	$2\,^3S$-$2\,^3P/1\,^1S$-$2\,^1S$	1.2293×10^{-13}
2.000	$2\,^3S$-$2\,^3P/1\,^1S$-$2\,^1S$	4.4138×10^{-13}
5.000	$2\,^3S$-$2\,^3P/1\,^1S$-$2\,^1S$	4.8762×10^{-12}
10.000	$2\,^3S$-$2\,^3P/1\,^1S$-$2\,^1S$	4.6078×10^{-11}
20.000	$2\,^3S$-$2\,^3P/1\,^1S$-$2\,^1S$	5.5648×10^{-10}
50.000	$2\,^3S$-$2\,^3P/1\,^1S$-$2\,^1S$	1.9496×10^{-8}
100.00	$2\,^3S$-$2\,^1P/1\,^1S$-$2\,^1S$	2.7815×10^{-7}

[a] For this and the following entries, the strongly forbidden $1\ ^1S - 2\ ^3S$ transition has a slightly lower limit.

Sensitivity of second-King transitions for Li^+ to NP for $n = 2$ and $\gamma = 0.001$ ($m_\phi = 11.1868$ eV).

King transitions	$y_e y_n \times 10^{15}$
$2\,^1S$-$2\,^3P/2\,^3S$-$2\,^1P$	115.16
$2\,^1S$-$2\,^3S/2\,^1P$-$2\,^3P$	118.19
$2\,^3S$-$2\,^1P/2\,^1P$-$2\,^3P$	131.18
$2\,^1S$-$2\,^3S/2\,^1S$-$2\,^3P$	143.23
$2\,^3S$-$2\,^3P/2\,^1P$-$2\,^3P$	165.30
$2\,^1S$-$2\,^3S/2\,^3S$-$2\,^3P$	165.40
$2\,^1S$-$2\,^3S/2\,^1S$-$2\,^1P$	168.01
$2\,^1S$-$2\,^1P/2\,^1P$-$2\,^3P$	169.65
$2\,^1S$-$2\,^3S/2\,^3S$-$2\,^1P$	202.20
$2\,^3S$-$2\,^1P/2\,^3S$-$2\,^3P$	205.17
$2\,^1S$-$2\,^3P/2\,^3S$-$2\,^3P$	216.48
$2\,^1S$-$2\,^3P/2\,^1P$-$2\,^3P$	221.65
$2\,^1S$-$2\,^1P/2\,^3S$-$2\,^1P$	258.26
$2\,^1S$-$2\,^1P/2\,^1S$-$2\,^3P$	268.51
$2\,^1S$-$2\,^1P/2\,^3S$-$2\,^3P$	13748.
Compare with	
$2\,^1S$-$10\,^1S/2\,^3P$-$10\,^1S$	9.631

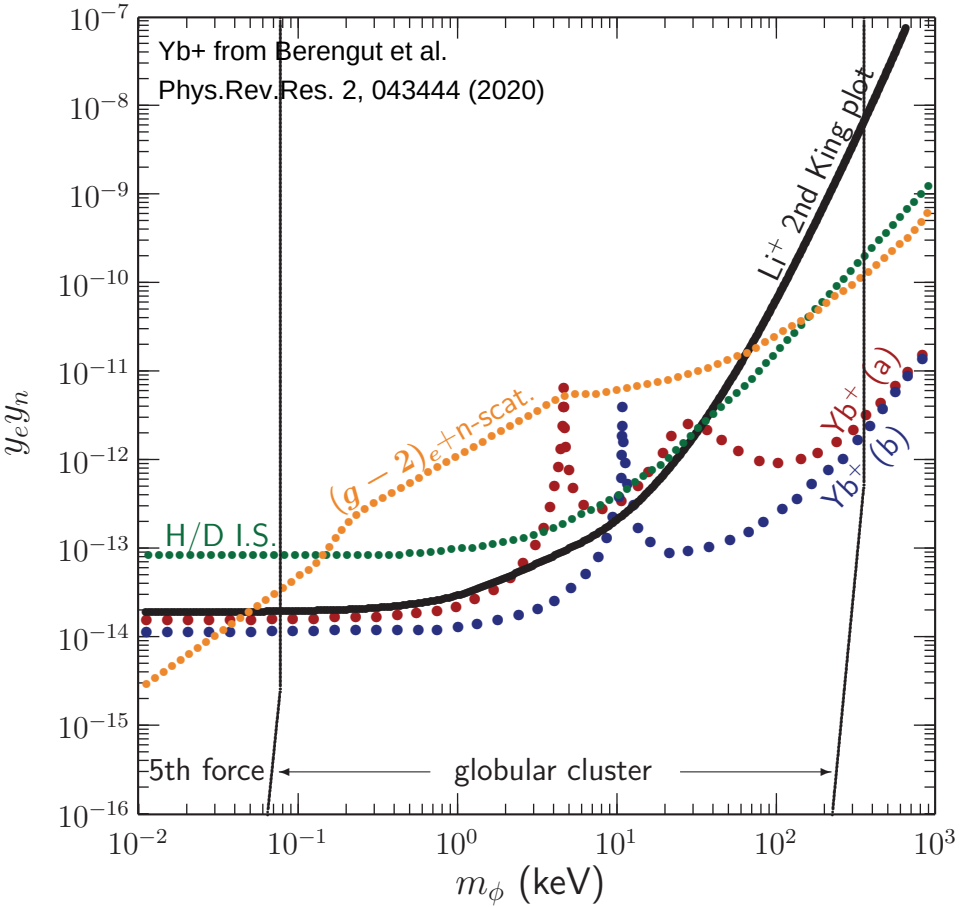
Yb+ from Berengut et al.
Phys.Rev.Res. 2, 043444 (2020)
Li+ 2nd King plot
(g − 2)e+n-scat.
H/D I.S.
Yb+ (a)
Yb+ (b)
5th force
globular cluster
$y_e y_n$
m_ϕ (keV)
10^{-7}
10^{-8}
10^{-9}
10^{-10}
10^{-11}
10^{-12}
10^{-13}
10^{-14}
10^{-15}
10^{-16}
10^{-2}
10^{-1}
10^{0}
10^{1}
10^{2}
10^{3}

Conclusions and Discussion

- We have defined and tested a second-King plot method that eliminates second-order mass shifts, as needed for light ions such as Li^+.
- We have carried out high-precision variational calculations for all states of Li^+ up to $n = 10$ and $L = 7$, and identified the ones most sensitive to a putative electron-neutron interaction, useful for boson masses up to about 10 keV.
- The sensitivity is about the same as for recent experiments involving Yb^+ for boson masses up to about 10 keV.
- The optimum King-plot combination is $2\,^1S$-$10\,^1S/2\,^3P$-$10\,^1S$ at 87.53 nm and 89.87 nm respectively.
- The $7I-10H$ transition at 2142 nm is a special case because of strong cancellation of the field shift (independent of Z).
- The same methods can be applied to helium and other light heliumlike ions.
- Online resources are available at http://drake.sharcnet ca.

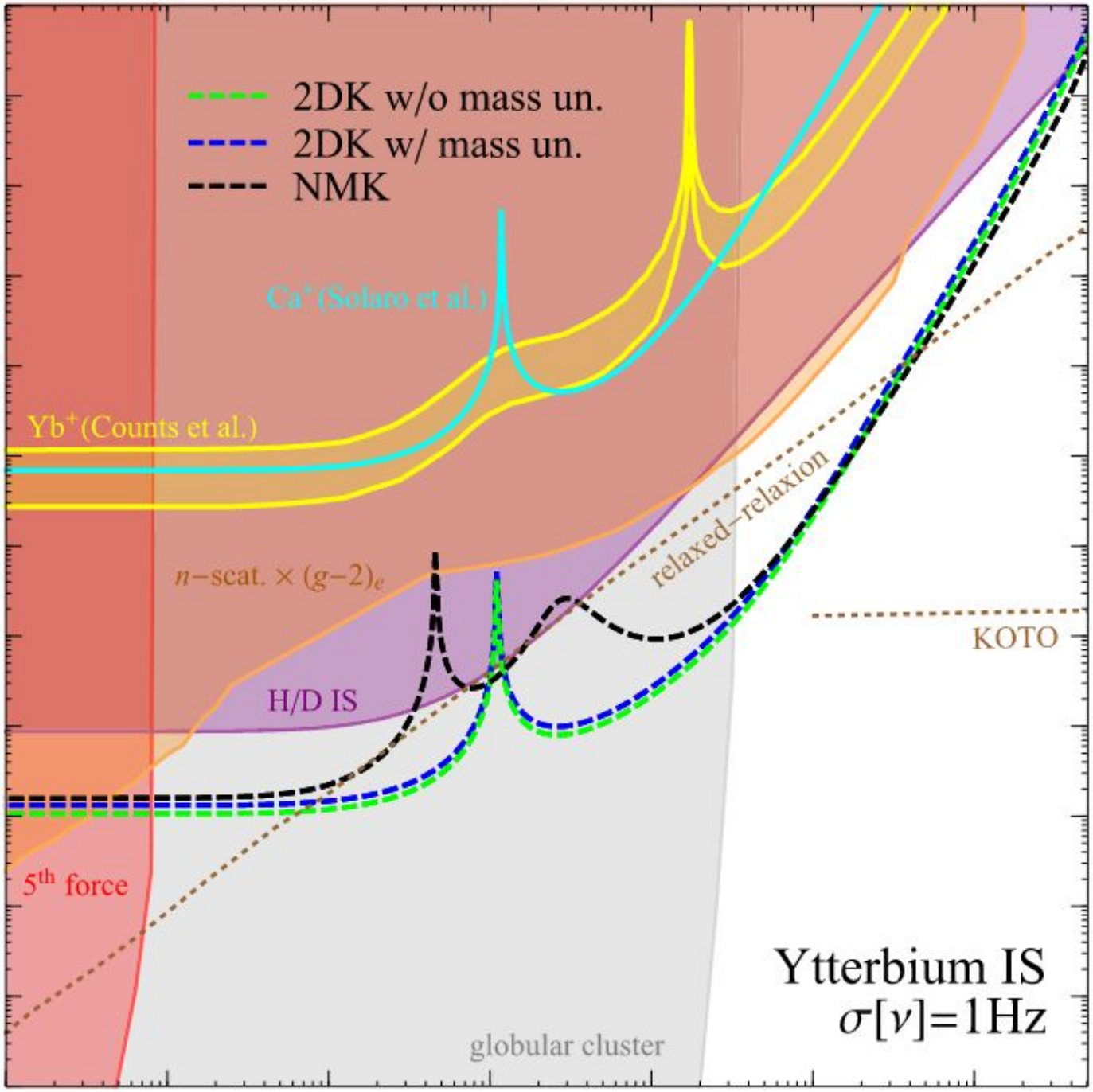
2DK w/o mass un.
2DK w/ mass un.
NMK
Ca+(Solaro et al.)
Yb+(Counts et al.)
n−scat. × (g−2)e
relaxed−relaxion
KOTO
H/D IS
5th force
globular cluster
Ytterbium IS
σ[ν]=1Hz